

# A study of zwitterionic/cationic vesicle formation and the influence of hyaluronan on this formation

Jana Burdíková<sup>1</sup> · Irena Solná<sup>1,2</sup> · Leoš Doskočil<sup>2</sup> · Filip Mravec<sup>1,2</sup> · Miloslav Pekař<sup>1,2</sup>

Received: 17 November 2016 / Revised: 15 February 2017 / Accepted: 16 April 2017 / Published online: 15 May 2017  
© Springer-Verlag Berlin Heidelberg 2017

**Abstract** The aggregation behavior of the biocompatible and naturally occurring zwitterionic phospholipid 1,2-dipalmitoyl-sn-glycero-3-phosphatidylcholine (DPPC) combined with its synthetic cationic analogue 1,2-dipalmitoyl-3-trimethylammonium-propan (DPTAP) was studied. Further, the physical properties of the formed DPPC/DPTAP liposomes were determined. The phase transition temperature of DPPC/DPTAP mixtures was studied using the steady-state fluorescence of laurdan, and the results were compared with those obtained from microcalorimetry measurements. The phase transition temperature was higher for all DPPC/DPTAP mixtures compared to that for pure DPPC and DPTAP, this increase being particularly pronounced for equimolar mixtures of DPPC and DPTAP. Membrane fluidity was determined by means of 1,6-diphenyl-1,3,5-hexatriene fluorescence anisotropy measurements. While the ratio of DPPC in DPPC/DPTAP liposomes was increased, the results suggest the formation of more tightly packed membranes. The interaction of DPPC/DPTAP liposomes with hyaluronan (Hya) was also studied. The formation of complexes was observed at a specific DPTAP/Hya concentration ratio independently of DPPC concentration or the molecular weight of Hya.

**Keywords** Liposome · Lipid · Phase transition temperature · Lipid order parameter · Fluidity · Hyaluronan

## Introduction

Liposomes are important delivery systems composed of lipid bilayers, which have considerable potential for application in medicine and cosmetics. Liposomes can undergo aggregation, fusion, and flocculation due to interactions with serum proteins under physiological conditions [1]. They have the capability to solubilize various forms of bioactives, regardless of hydrophilicity. Bioactives soluble in water can be loaded into hydrophilic regions while hydrophobic therapeutics can be captured in lipid regions at high densities. Lipid encapsulation can provide protection of the loaded bioactive from harsh environmental conditions and limits systemic exposure, which is advantageous in the case of therapeutics having undesired cytotoxic side effects [2]. Cationic liposomes have been shown to be absorbed by immature vascular endothelial cells due to the negative electric charge of their outer cell membrane. The antitumor efficacy of paclitaxel encapsulated in cationic liposomes was demonstrated as a promising new method for the treatment of prostate cancer reducing the primary tumor mass [3].

The instability of membrane conformation, which is essential to the delivery function of liposomes, could be improved by inclusion of a helper lipid. Stable and relatively small unilamellar vesicles were obtained by the insertion of lipid with cationic head groups such as 1,2-dioleoyl-3-trimethylammonium-propan (DOTAP) in zwitterionic phosphatidylcholine (PC) membranes [4]. The mixture of 1,2-dipalmitoyl-sn-glycero-3-phosphatidylcholine (DPPC) and 1,2-dipalmitoyl-3-trimethylammonium-propan (DPTAP) is widely used in a variety of applications, e.g., for the formation of lipoparticles [5, 6] or the coating of superparamagnetic iron oxide nanoparticles

**Electronic supplementary material** The online version of this article (doi:10.1007/s00396-017-4103-z) contains supplementary material, which is available to authorized users.

✉ Jana Burdíková  
xcszewieczkovaj@fch.vutbr.cz

- <sup>1</sup> Institute of Physical and Applied Chemistry, Faculty of Chemistry, Brno University of Technology, Purkynova 118/464, 612 00 Brno, Czech Republic
- <sup>2</sup> Materials Research Centre, Faculty of Chemistry, Brno University of Technology, Purkynova 118/464, 612 00 Brno, Czech Republic

[7]. The proportion of each one in the formulation controls the cationic charge of the vesicle surface [8]. Independently of DPPC/DPTAP molar ratios, DPPC and DPTAP spontaneously assemble into vesicles in water media. Significant electrostatic interactions between lipids can be demonstrated by a higher phase transition temperature compared to that of pure lipids. The strongest interactions were found in the case of equimolar mixtures of DPPC and DPTAP revealing the tightest packing density of lipids [9].

Phospholipids are in the gel or liquid crystalline phase at physiological temperature. The DPPC phase transition temperature is around 41.5 °C and can be modified by the incorporation of other lipids. This change in phase transition temperature depends both on the length and saturation of the acyl chain and the type of polar residues [10]. For example, the incorporation of DOTAP into DPPC membranes causes a decrease in its phase transition temperature [4], while DPTAP has the opposite effect [9]. For steady-state fluorescence research into phase transition temperature, the prodan derivative laurdan can be utilized, this containing the lauric acid tail; this compound is thus tightly anchored within the hydrophobic core by cooperative van der Waals interactions between the lauric acid tail and the lipid hydrocarbon chains [11]. Due to the presence of naphthalene moiety, it is sensitive to both the polarity of the local environment and the membrane phase state [12, 13]. The essence of this sensitivity to polarity is subsumed in the partial charge separation between the 2-dimethylamino and 6-carbonyl residues forming a dipole moment, which increases upon excitation and may cause reorientation of the surrounding solvent dipoles. This solvent reorientation consumes energy and decreases the probe's excited state energy resulting in a continuous red shift of the probe's emission spectrum [12, 14]. Thus, the red shift in laurdan emission spectra indicates the increased concentration of water in the bilayer and its increased mobility [12].

Fluorescence anisotropy can be utilized for the investigation of lipid order. For this purpose, the fluorescent probe 1,6-diphenyl-1,3,5-hexatriene (DPH) allows information about the degree of membrane fluidity or physical changes in membranes to be obtained on the basis of the determination of the molecular orientational order and reorientational dynamics of the fluorescent probe in the core of the membrane bilayer [15, 16]. DPH is a rather rigid, linear, rod-like fluorophore characterized by an absence of polar groups; therefore, it is distributed spontaneously into the hydrophobic acyl chain region of the membrane [17], oriented such that the long axis of DPH along its rod-like shape is approximately aligned normal to the bilayer, thus reflecting the ordering of lipid acyl chains [17, 18]. The fluorescence anisotropy of DPH works well for studies of membrane fluidity in systems that are in the liquid-disordered phase. In the liquid-ordered phase, the fluorescence anisotropy of DPH serves well as a qualitative tool, while the quantitative accuracy is limited [19].

Hyaluronan (Hya) is a carbohydrate polymer occurring naturally in all living organisms. Hya is a linear, unbranched polymer, which is composed of a repeating disaccharide structure [20]. It can be several thousands of disaccharide units long [21] but can also exist as small fragments or oligosaccharides. At physiological pH, Hya exists mostly as a sodium salt and is therefore highly charged. This highly charged nature of Hya provides its solubility and ability to bind water extensively [22]. Hya plays a critical role in the physiology of joint function, including lubrication of the synovial surfaces. Interactions between Hya and phospholipids were studied as a simplified model of synovial fluid. Phospholipids could facilitate Hya binding to cells due to its strong affinity to cell surfaces. A complex of Hya and phospholipids (Haplex) was prepared using the film dispersion and sonication method, resulting in the enhancement of the oral absorption of Hya [23]. After the addition of Hya to monolamellar or multilamellar phospholipid suspensions, phospholipid organization was significantly affected by the presence of Hya in dependence on its molecular weight, not by the initial organization of the phospholipid or its nature (DPPC or egg lecithin) [24]. The presence of liposomes (DPPC) leads to an abrupt decrease in the viscosity of Hya because DPPC membranes bound to Hya cause the collapse of Hya chains. The possible explanation is that DPPC membranes bind to hydrophobic "patches" situated along the Hya polymer resulting in the collapse of the Hya chain [25, 26].

This work is aimed at preparation and characterization of DPPC/DPTAP vesicles with positive charge and study of their interactions with negatively charged Hya.

## Experimental section

### Materials

Sodium hyaluronate (137, 458, 1697 kDa) was purchased from Contipro (Czech Republic); 1,2-dipalmitoyl-3-trimethylammonium-propan, chloride salt (DPTAP) was purchased from Avanti Polar Lipids. 1,2-Dipalmitoyl-sn-glycero-3-phosphatidylcholine (DPPC), 1,6-diphenyl-1,3,5-hexatriene (DPH), pyrene, and chloroform were purchased from Fluka. All experiments were performed in water purified by an ELGA lab system (PURELAB flex).

### Vesicle formation

The required amount of DPTAP or DPPC and DPTAP (with molar ratios 0:100, 50:50, 75:25, 80:20, 90:10) was dissolved in chloroform. After the removal of chloroform by evaporation, the required amount of water was added and the solution was sonicated at a temperature above the phase transition temperature until opalescent.

## Microcalorimetry measurements

Microcalorimetry studies were conducted using a TAM III thermal activity monitor (TA Instruments, New Castle, DE, USA). Two-and-a-half-gram lipid or lipid mixture samples prepared as described previously in vesicle formation (with a total lipid concentration of 2.7 mM) were placed into disposable crimp seal ampoules. Samples were equilibrated for 15 min at 25 °C. The scanning rate was set to 2 °C/h. Any heat generated or absorbed by the sample was measured continuously over time. Measurements were carried out in the temperature range 25–65 °C. The baseline was subtracted.

## Samples for fluorescence measurements

A fluorescence probe (laurdan, DPH, pyrene) dissolved in acetone was added to vials. After the evaporation of acetone under reduced pressure, an increasing amount of DPTAP or DPPC/DPTAP bulk solution and water was added into the vials to achieve a DPTAP or DPPC/DPTAP concentration series (in the range of  $10^{-4}$ –1 mM) or to achieve a specific lipid concentration (in the case of samples containing laurdan or DPH). Eventually, a given amount of Hya bulk solution was added. Samples were measured after 24 h of agitation.

## Laurdan generalized polarization

The characteristics of the laurdan emission spectrum describing the presence/absence of water molecules in the vicinity of laurdan naphthalene moiety may be expressed by the generalized emission polarization (GP) value [10, 27] given by the following:

$$GP = \frac{I_{440} - I_{490}}{I_{440} + I_{490}}$$

where  $I_{440}$  and  $I_{490}$  are the fluorescence intensities measured at 440 and 490 nm [10, 12], the wavelengths at which laurdan emission maxima occur in the gel phase and in the liquid crystalline phase, respectively [12, 14]. The phase transition temperature was determined from the first intersection of straight-line segments fitting plots of the laurdan GP value versus temperature.

All steady-state fluorescence measurements were performed using a Fluorolog Horiba Jobin Yvon spectrofluorimeter. Laurdan emission spectra were collected in the range 380–550 nm using an excitation wavelength of 329 nm. All samples were measured as a function of temperature in the range 35–65 °C or wider when necessary. Temperature was controlled by a circulating water bath. Sample temperature homogeneity was maintained by magnetic stirring.

## Phospholipid CAC determination

For samples containing pyrene as a fluorescence probe, excitation spectra (in the range 330–340 nm with an emission wavelength of 392 nm) and emission spectra (in the range 360–540 nm with an excitation wavelength of 335 nm) were measured. The emission polarity index (EmPI) was obtained from the emission spectrum by dividing the fluorescence intensity of the first emission band (373 nm) by that of the third emission band (383 nm). The excimer to monomer (Ex/Mo) ratio was determined by dividing the fluorescence intensity of the excimer band (470 nm) by that of the monomer (383 nm) band. The excitation polarity index (ExPI) was calculated from excitation spectra as the ratio of fluorescence intensities at 333 and 338 nm. The dependences of EmPI (or ExPI) on lipid concentration were analyzed using the OriginLab software by fitting a Boltzmann sigmoid with the following form:

$$y = \frac{A_1 - A_2}{1 + e^{\frac{x-x_0}{\Delta x}}} + A_2$$

where  $y$  corresponds to EmPI or ExPI,  $A_1$  and  $A_2$  are the upper and lower limits of the sigmoidal curve, the independent variable  $x$  represents the total concentration of surfactant,  $x_0$  represents the point of inflection, and  $\Delta x$  is the gradient at which the step change takes place. Critical concentrations of aggregation (CACs) were obtained as the point of inflection ( $x_0$ ).

## Anisotropy of DPH determination

Samples were prepared as described earlier in “Samples for fluorescence measurements” section. The concentration of the DPPC/DPTAP mixture was above the concentration corresponding to the second break in the sigmoidal curve. DPH anisotropy was measured using a time-resolved fluorescence spectrometer (FluoroCube Horiba). Samples were excited at 372 nm using a laser diode with an appropriate filter, and the DPH emission was measured at 426 nm with the slit adjusted to 8 nm.

For each vesicle composition with different DPPC/DPTAP ratios, fluorescence intensities were measured under four separate polarizer conditions:  $I_{vh}$  (vertically polarized excitation and horizontally polarized emission),  $I_{vv}$  (vertically polarized excitation and emission),  $I_{hh}$  (horizontally polarized excitation and emission), and  $I_{hv}$  (horizontally polarized excitation and emission).

These intensities were then fitted by impulse reconvolution using the general equation:

$$F(t) = R(\text{inf}) + B_i \exp\left(\frac{-t}{\tau_i}\right)$$

where  $R(\text{inf})$  corresponds to the intrinsic anisotropy,  $t$  is the fluorescence lifetime,  $\tau_i$  is the rotational correlation time, and

$B_i$  a pre-exponential factor. The actual DPH fluorescence decay ( $I(t)$ ) is assumed to follow a double exponential model:

$$I(t) = R(\text{inf}) + B_1 \exp\left(\frac{-t}{\tau_1}\right) + B_2 \exp\left(\frac{-t}{\tau_2}\right)$$

Then, the  $G$ -factor was calculated as the average value of the intensity ratio to minimize the consequences of the fact that monochromators do not transmit polarized components of light equally.

$$G = \frac{I_{hv}(t)}{I_{hh}(t)}$$

Using the  $G$ -factor and intensity values, the anisotropy  $r(t)$  was then calculated according to the relationship:

$$r(t) = \frac{I_{vv}(t) - GI_{vh}(t)}{I_{vv}(t) + 2GI_{vh}(t)}$$

### Lipid order parameter calculation

The lipid order parameter ( $S$ ) and effective lipid order parameter ( $S_{\text{eff}}$ ) were calculated using values of fluorescence anisotropy as follows [28, 29]:

$$S = \left(\frac{r}{r_0}\right)^{1/2}, S_{\text{eff}} = \left(\frac{r}{0.4}\right)^{1/2}$$

where  $r$  is the observed anisotropy and  $r_0$  is the intrinsic anisotropy of the molecule. The term  $r_0$  is used to refer to the anisotropy observed in the absence of other depolarizing processes such as rotational diffusion or energy transfer. For DPH,  $r_0$  values as high as 0.39 have been measured. The anisotropy of 0.39 corresponds to an angle of  $7.4^\circ$  between the dipoles, whereas an  $r_0$  value of 0.4 corresponds to an angle of  $0^\circ$  [30].

## Results and discussion

The phase transition temperature was studied by means of fluorescence spectroscopy and microcalorimetry. The results of microcalorimetry measurements are shown in Fig. 1. A sharp phase transition is clearly observable in the case of pure lipids (DPPC, DPTAP) and mixtures with a DPPC/DPTAP ratio of 50:50. The phase transition temperatures for DPPC and DPTAP are localized at 42 and 43 °C, respectively, while it moves to higher temperatures in the case of mixed vesicles prepared from these two lipids. The highest phase transition temperature was found for a mixture with a DPPC/DPTAP ratio of 50:50 and was localized approximately at 57 °C. The reason for the shift of the phase transition temperature

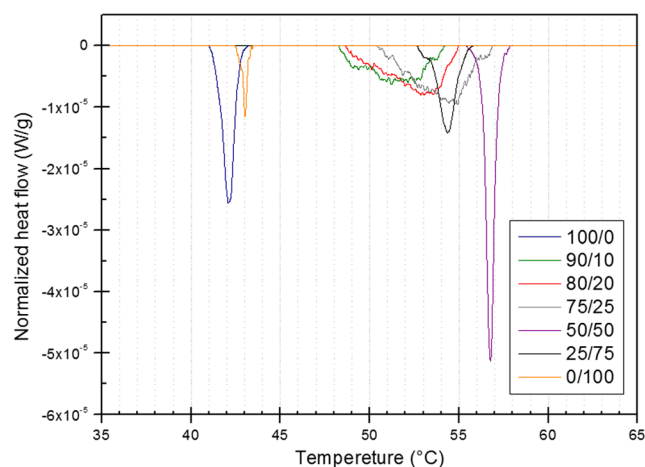


**Fig. 1** Normalized heat flow in DPPC/DPTAP vesicles

to higher values in the case of all DPPC/DPTAP mixtures probably lies in the DPPC headgroup dipole orientation resulting from the presence of DPTAP. Charge repulsion between DPTAP and the terminal  $N^+(\text{CH}_3)_3$  group in DPPC hinders the dipole reorientation that accompanies melting (from perpendicular to the interface to parallel to the interface) and prolongs the gel phase [7].

The dependences of normalized heat flow on temperature corresponding to DPPC/DPTAP mixtures with an excess of DPPC (90:10, 80:20, and 75:25) are noticeably broader than the others. Vesicles of these compositions are probably not homogenous through the entire sample volume; thus, they do not exhibit a sharp phase transition, but rather a continuous one.

The spectral shifts with increasing temperature in laurdan emission spectra were quantified using generalized polarization (GP) values. GPs as a function of temperature are shown in Fig. 2 and have a sigmoid character for all studied mixtures. We observed the same character in all dependencies—a slight

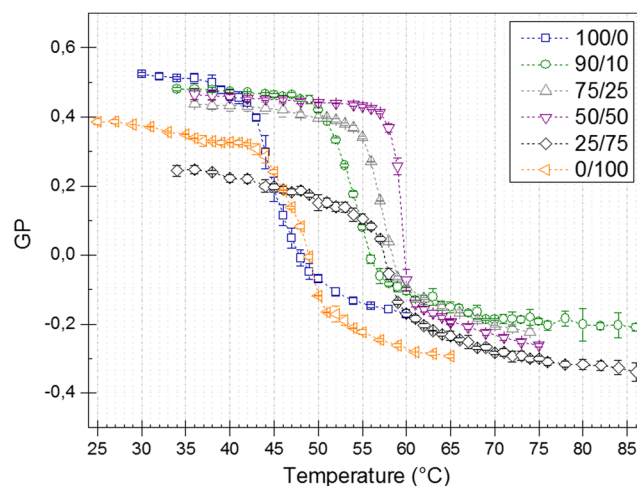


**Fig. 2** Laurdan generalized polarization (GP) as a function of temperature in DPPC/DPTAP vesicles



decrease in GP in the first stage, followed by sharp GP decline, and then a further slight decrease in GP at the end. We quantified the differences between the location and slope of the intermediate area, which are both summarized and compared with results obtained by microcalorimetry in Fig. 3. The small deviation between the obtained results can be explained on the basis of the different principles of these two techniques. The phase transition temperature was higher for all studied mixtures compared to that for pure lipids, this increase being the highest for the equimolar DPPC/DPTAP mixture.

It is worth noting the low values of GP at low temperatures for mixtures with DPPC/DPTAP ratios of 25:75 and 0:100. According to the literature, GP ranges from  $-0.3$  to  $0.3$  for the liquid phase of lipid bilayers and from  $0.5$  to  $0.6$  for the gel phase [12, 14]. According to these values, mixtures consisting mainly of DPTAP should not be in the gel state. However, if we consider the essence of GP, the decrease in GP is caused by an increase in the laurdan emission band located at around  $490$  nm, resulting from an increased polar head group area and the presence of some water molecules in the vicinity of laurdan naphthalene moiety, this indicating a larger head group area per molecule as a consequence of repulsion due to the presence of the positive charge located at the trimethylammonium group.

Another point of interest is the slope of the rapidly decreasing part in the dependences of GP on temperature. Figures 2 and 3 clearly show that all dependences have nearly the same slope for the intermediate part, except for the mixture with a DPPC/DPTAP ratio of 50:50, where the slope is doubled. This high slope could indicate the fastest transition from gel to liquid crystalline phase, as observed in microcalorimetry experiments.

This observation suggests tightly packed membranes, as was observed in equimolar dimyristoylphosphatidylcholine (DMPC)/dimyristoyltrimethylammonium propane (DMTAP) mixtures [31].

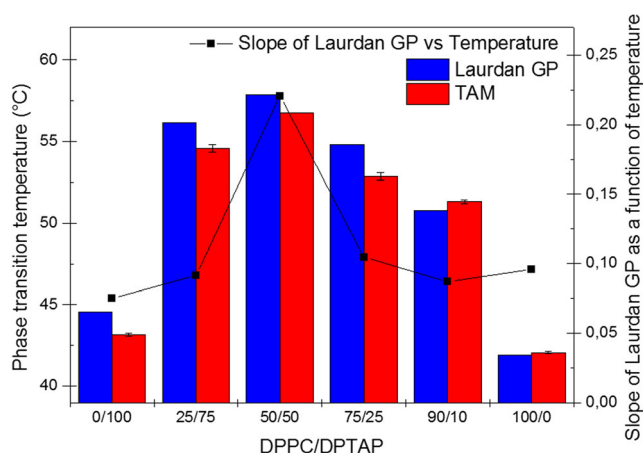


**Fig. 3** Phase transition temperature in DPPC/DPTAP vesicles obtained using laurdan generalized polarization and microcalorimetry and the slope (absolute value) of the dependence of laurdan GP on temperature

## Lipid order parameter

The change in the order of the lipid membrane was expressed by the effective lipid order parameter ( $S_{\text{eff}}$ ), determined from the anisotropy of DPH fluorescence measurements. All measured values (Fig. 4) were higher than those reported in literature for different membrane constructs formed by 16:0–18:1 PC and cholesterol [28]. The reason for the high measured values probably lies in the presence of only one acyl chain type in each lipid, forming a relatively ordered membrane. The  $S_{\text{eff}}$  values increased slightly with the increasing proportion of DPPC in the DPPC/DPTAP mixture. This gentle fluidization of membranes at low DPPC portions may be caused by repulsive forces between positively charged DPTAP head groups, which are suppressed by an increasing amount of DPPC in the mixture. This would be in good agreement with the low values of laurdan GP obtained with high proportions of DPTAP.

These results are in agreement with literature, where the increase of hydration of the lipid headgroup region was observed with increasing DMTAP portion in DMPC/DMTAP system, because pure TAP membranes are less packed [32].

## Aggregation of DPTAP with Hya

To study the influence of Hya on DPTAP aggregation, we used Hya of different concentrations and molecular weights (137, 458, 1697 kDa). On systems containing pyrene as a fluorescence probe, we measured steady-state fluorescence excitation and emission spectra and obtained EmPI (and ExPI) as described earlier.

The dependencies of pyrene EmPI on DPTAP concentration for pure DPTAP and its mixtures with Hya of different concentrations (5, 15, 50, 100, and 1000  $\text{mg dm}^{-3}$ ) and a molecular weight of 458 kDa are shown in Fig. 5. The

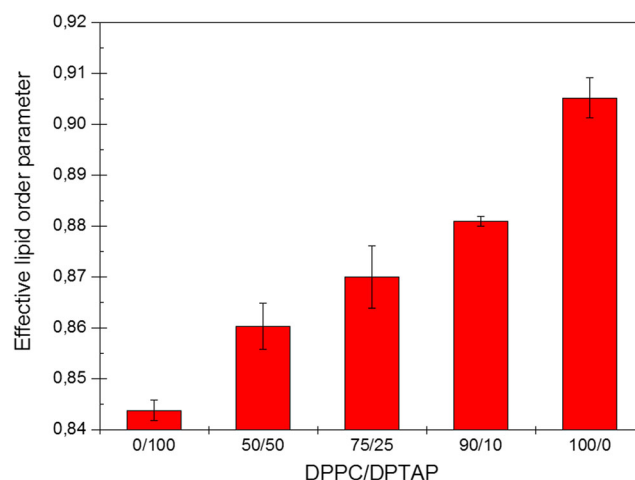
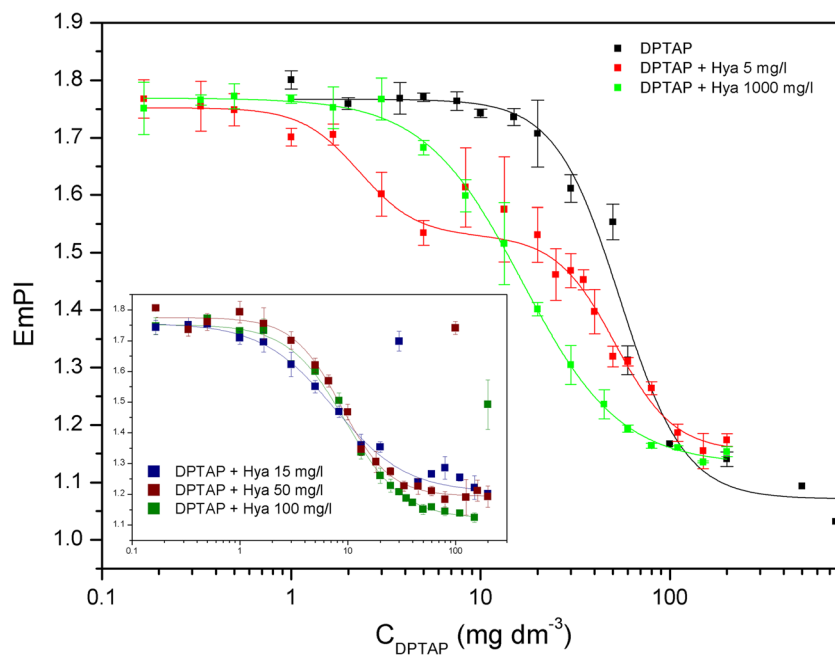


**Fig. 4** Detail of the effective lipid order parameter of DPPC/DPTAP vesicles with different DPPC/DPTAP ratios

**Fig. 5** Dependence of pyrene EmPI on DPTAP concentration for DPTAP and its mixtures with Hya of different concentrations and the same molecular weight of 458 kDa



dependence corresponding to DPTAP has a sigmoid character, with high EmPI values at low DPTAP concentrations indicating fluorescence from a polar (water) environment. At high DPTAP concentrations, EmPI values are low, because fluorescence occurs from the hydrophobic region.

In the presence of Hya, a reincrease in pyrene EmPI was observed at a DPTAP concentration dependent on the concentration of Hya, not only a smooth decrease in pyrene EmPI as observed in the case of pure DPTAP. This pyrene EmPI reincrease was accompanied by the formation of precipitate. From this behavior, we can suggest that almost all lipids in the sample are consumed for precipitate formation. Thus, a small amount of lipids remains in the solution, and high values of EmPI are found. The measured values of CAC for systems containing DPTAP and Hya are listed in Table 1. The

parameters of pyrene EmPI reincrease are also shown. Values of the  $C_{\text{DPTAP}}/C_{\text{Hya}}$  ratio were 1.67 or 2.00. It can be said, with regard to the number of samples and the concentration step, that the  $C_{\text{DPTAP}}/C_{\text{Hya}}$  ratio of the EmPI increase is always the same (approaching a value of 2). No reincrease in EmPI was observed at the Hya concentration of 1000  $\text{mg dm}^{-3}$ , because this concentration of Hya was too high to achieve a  $C_{\text{DPTAP}}/C_{\text{Hya}}$  ratio of “2.” In contrast, a double Boltzmann sigmoid was used to fit the data obtained at the Hya concentration of 5  $\text{mg dm}^{-3}$ . The concentration of the first point of inflection was lower than that at the Hya concentration of 15  $\text{mg dm}^{-3}$ , and the concentration of the second point of inflection was nearly the same as CAC in the case of pure DPTAP. This may be a result of the mixture separating into two different systems, one of which contains a

**Table 1** Measured values of CAC of DPTAP mixtures with Hya of different concentrations and molecular weights and parameters of pyrene EmPI reincrease

Hya		CAC ( $\text{mg dm}^{-3}$ )	Pyrene EmPI reincrease	
$M_w$ (kDa)	$c$ ( $\text{mg dm}^{-3}$ )	EmPI	$C_{\text{DPTAP}}$ ( $\text{mg dm}^{-3}$ )	$C_{\text{DPTAP}}/C_{\text{Hya}}$ ( $\text{mg dm}^{-3}$ )
–	–	$52.7 \pm 3.1$	–	–
137	15	$5.2 \pm 0.2$	25	1.67
458	5	$4.5 \pm 0.2$	8.33	1.67
		$55.9 \pm 2.5^a$		
	15	$7.8 \pm 1.4$	30	2.00
	50	$8.9 \pm 0.1$	100	2.00
	100	$9.6 \pm 0.7$	200	2.00
	1000	$18.3 \pm 0.1$	–	–
1697	15	$6.0 \pm 0.7$	25	1.67

<sup>a</sup> Parameter of the point of inflection of the second Boltzmann sigmoid

predominant amount of Hya, while the other behaves rather like pure DPTAP. A second explanation could be that the DPTAP concentration (for a  $C_{\text{DPTAP}}/C_{\text{Hya}}$  ratio of 2 and the Hya concentration of  $5 \text{ mg dm}^{-3}$ ) is too low to form vesicles which should interact with Hya and form a precipitate.

The aggregation was also observed in the case of cationic liposomes (EPC/DOPE/DOTAP) and low molecular weight Hya. The increase of size of aggregates occurs in the concentration range of Hya 3 to 20% [33].

The values of CAC for DPTAP mixtures with Hya of different concentrations and a molecular weight of 458 kDa obtained using EmPI are also graphically depicted in Fig. 6. As can be clearly seen, a slight increase in CAC was observed with increasing Hya concentration but was not as pronounced as that obtained in the case of pure DPTAP. For the mixture of DPTAP with Hya of concentration  $5 \text{ mg dm}^{-3}$ , two values of CAC are shown, as described earlier.

The reincrease in EmPI (and also ExPI) was accompanied visually by the formation of precipitate on the wall of the vial (Fig. S1). Only in the case of samples with the Hya concentration of  $50 \text{ mg dm}^{-3}$  was the precipitate formed at a three times lower concentration than the concentration at which an increase in EmPI occurred. In this case, the appearance of the formed precipitate was different. Then, samples with higher DPTAP and Hya concentrations were prepared, the  $C_{\text{DPTAP}}/C_{\text{Hya}}$  ratio remaining at 2 (Fig. S2).

The dependencies of pyrene ExPI on DPTAP concentration (not shown) had a similar character to those of EmPI on DPTAP concentration; only slightly lower CACs values were obtained.

In addition, the influence of the molecular weight of Hya on precipitate formation with DPTAP was studied. Three

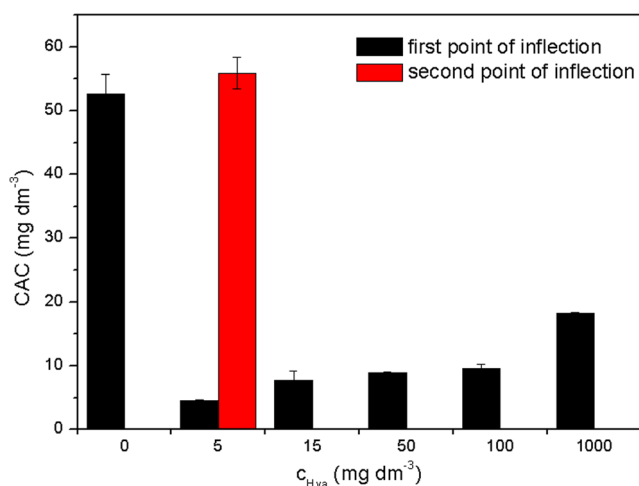


**Fig. 6** CAC of DPTAP and Hya mixtures with different Hya concentrations determined by pyrene EmPI. In the case of a Hya concentration of  $5 \text{ mg dm}^{-3}$ , a double Boltzmann curve was used to fit the dependence of pyrene EmPI on DPTAP concentration, and two points of inflection were obtained

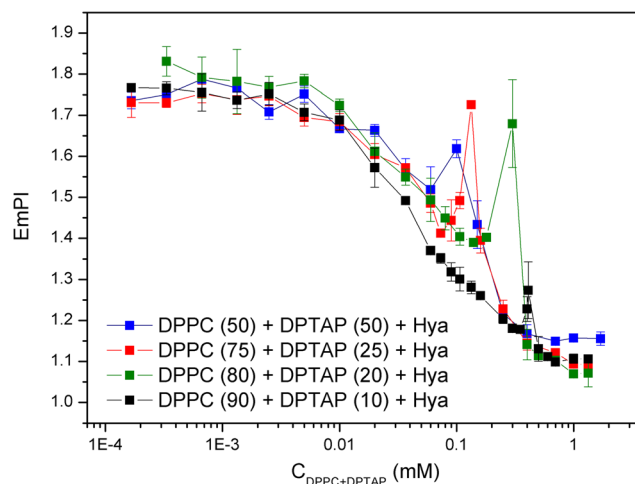


**Fig. 7** Dependence of pyrene EmPI on DPPC and DPTAP concentration for different DPPC/DPTAP ratios in the presence of Hya ( $15 \text{ mg dm}^{-3}$ , 458 kDa)

molecular weights of Hya were used (137, 458, and 1697 kDa), and its concentration was  $15 \text{ mg dm}^{-3}$  in all cases. No influence of Hya molecular weight was observed (see Fig. S3), and the measured values of CAC were nearly the same (Table 1). An abrupt increase in pyrene EmPI (and also ExPI) was observed in all cases at the same concentrations, and the formed precipitate had the same appearance.

#### Aggregation of DPPC/DPTAP mixture in the presence of Hya

Four mixtures with different DPPC/DPTAP molar ratios (50:50, 75:25, 80:20, and 90:10) were prepared to study the effect of Hya on DPPC/DPTAP aggregation. In the case of the DPPC/DPTAP mixture with a molar ratio of 50:50, the results

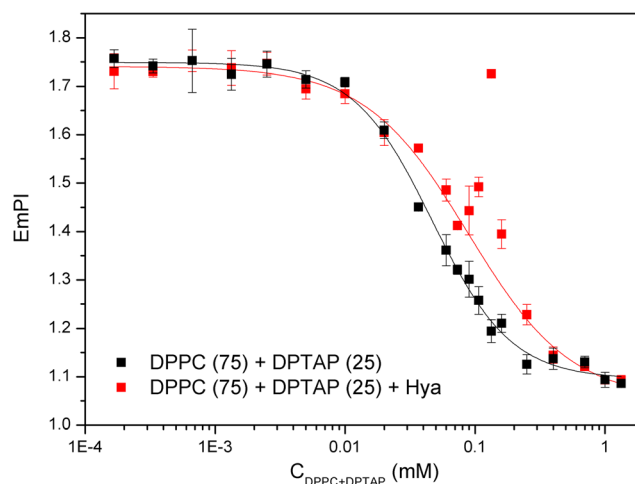


**Fig. 8** Dependence of pyrene EmPI on DPPC and DPTAP concentration for a DPPC/DPTAP ratio of 75:25 in the presence and absence of Hya ( $15 \text{ mg dm}^{-3}$ , 458 kDa)

**Table 2** Measured values of the CAC of DPPC/DPTAP mixtures with Hya (15 mg dm<sup>-3</sup>, 458 kDa) and the parameters of breaks in the Boltzmann curve of DPPC/DPTAP mixtures with Hya

DPPC/ DPTAP	CAC (μM)		Break		C <sub>DPPC</sub> / C <sub>Hya</sub> (mg dm <sup>-3</sup> )	C <sub>DPTAP</sub> (μM)	C <sub>DPTAP</sub> (mg dm <sup>-3</sup> )	C <sub>DPTAP</sub> /C <sub>Hya</sub> (mg dm <sup>-3</sup> )
	DPPC + DPTAP	DPPC	DPTAP	C <sub>DPTAP</sub>				
50:50	57 ± 2	28.65	28.65	28.65	—	—	—	—
50:50 Hya	85 ± 14	42.4	42.4	42.4	36.70	50	32.32	2.15
75:25	47 ± 4	35.2	11.8	11.8	—	—	—	—
75:25 Hya	86 ± 3	64.6	21.5	21.5	73.22	100	21.50	1.43
80:20	53 ± 2	42.3	10.5	10.5	—	—	—	—
80:20 Hya	134 ± 28	107.0	26.8	26.8	176.17	240	38.79	2.59
90:10	31 ± 2	27.6	3.1	3.1	—	—	—	—
90:10 Hya	52 ± 1	46.6	5.2	5.2	270.86	369	26.51	1.77

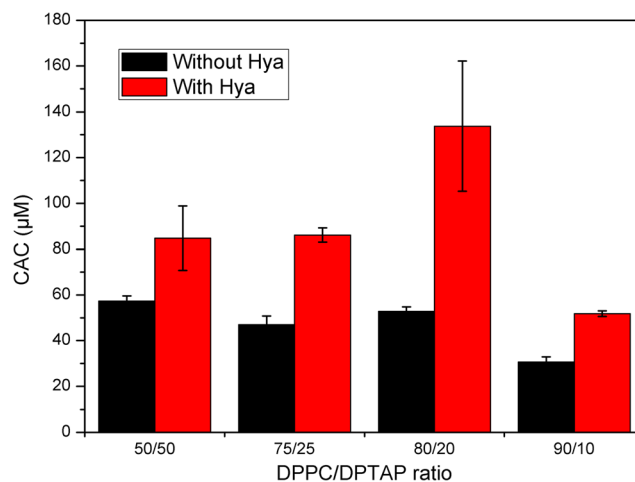
show that the molecular weight of Hya had no influence on either the dependence of EmPI on DPPC/DPTAP concentration (not shown) or CAC values (see Table S1). Therefore, further experiments were focused only on Hya of middle molecular weight (458 kDa).

Figure 7 compares the dependencies of EmPI on DPPC/DPTAP concentration as a function of different DPPC/DPTAP ratios. It is obvious that with a decreasing DPTAP ratio in the mixture, the reincrease in pyrene EmPI is localized at higher DPPC/DPTAP concentrations. Figure 8 shows an example of the dependences of EmPI on DPPC and DPTAP concentration (for a DPPC/DPTAP molar ratio 75:25) with and without Hya (of concentration 15 mg dm<sup>-3</sup> and molecular weight 458 kDa). After the addition of Hya, a reincrease in EmPI was observed (similarly as in the case of DPTAP and Hya mixtures); however, CAC values increased for all DPPC and DPTAP mixtures (Table 2, Fig. 9), which was in contrast to the addition of Hya to DPTAP, when CAC values decreased by approximately ten times.

Even here, we monitored the parameters when the reincrease in pyrene EmPI was observed. Similarly as in the case of DPTAP mixtures with Hya, we monitored the concentration ratio,  $C_{DPTAP}/C_{Hya}$ , and, moreover,  $C_{DPPC}/C_{Hya}$  (Table 2).

$C_{DPPC}/C_{Hya}$  ratio increases with decreasing portion of DPPC in DPPC/DPTAP mixture with Hya; therefore, the dependence of  $C_{DPPC}/C_{Hya}$  ratio on DPPC/DPTAP ratio is rather inconclusive.

Vice versa, the  $C_{DPTAP}/C_{Hya}$  ratio approached a value of 2 for all DPTAP and DPPC mixtures with Hya. It should be noted that the  $C_{DPTAP}/C_{Hya}$  ratio was also equal to 2 in the case of DPTAP/Hya mixtures (Table 1). Thus, aggregation is evidently controlled by the DPTAP concentration and  $C_{DPTAP}/C_{Hya}$  concentration ratios. It seems that the presence

**Fig. 9** Concentration of DPTAP and DPPC at the CAC (determined by pyrene EmPI) of various DPPC and DPTAP mixtures with Hya (15 mg dm<sup>-3</sup>, 458 kDa)



of DPPC does not affect the aggregation behavior of these systems, although the concentration of DPTAP at the CAC value of the DPPC/DPTAP/Hya mixture decreases with a decreasing amount of DPTAP in these mixtures (Fig. 9). The concentration of DPPC at the CAC of these mixtures shows no dependence on DPPC/DPTAP ratio (Fig. 9). Therefore, we can say that DPPC participates in the formation of DPPC/DPTAP/Hya aggregates but does not affect this formation directly.

After the addition of higher concentration of Hya (1000 mg dm<sup>-3</sup>), no reincrease in EmPI was observed and the influence on CAC values was insignificant.

## Conclusion

In this work, we studied the influence of Hya on vesicles formed by DPTAP and DPPC/DPTAP mixtures. The formation of vesicles and their interactions with Hya was confirmed by fluorescence spectroscopy. In case of DPTAP, the presence of Hya caused the significant decrease of CAC of the system. On the other hand, in DPPC/DPTAP mixed system, addition of Hya resulted in only slight decrease of CAC of the studied system independently on DPPC/DPTAP ratio. In addition, the interaction between studied lipid systems caused the formation of precipitate, which was controlled only by the DPTAP concentration, even in the case of DPPC/DPTAP mixtures with Hya. The precipitate was formed after reaching a specific DPTAP/Hya ratio, not only in the case of DPTAP and Hya mixtures, but also in the case of DPPC, DPTAP and Hya mixtures. Thus, the formation of precipitate is managed by DPTAP. We also focused on the study of DPPC/DPTAP membrane properties. Membrane fluidity was studied by means of the fluorescence anisotropy of DPH. It was shown that with an increasing proportion of DPPC, the DPPC/DPTAP membrane was more rigid. Phase transition was studied by laurdan steady-state fluorescence and microcalorimetry. The phase transition temperature was shown to increase for mixtures of DPPC/DPTAP, this increase being particularly pronounced for an equimolar mixture of DPPC and DPTAP.

CAC, critical concentration of aggregation; DOTAP, 1,2-dioleoyl-3-trimethylammonium-propan; DPH, 1,6-diphenyl-1,3,5-hexatriene; DPPC, 1,2-dipalmitoyl-sn-glycero-3-phosphatidylcholine; DPTAP, 1,2-dipalmitoyl-3-trimethylammonium-propan; EmPI, emission polarity index; ExPI, excitation polarity index; GP, generalized polarization; Hya, hyaluronan; PC, phosphatidylcholine; S, lipid order parameter; Seff, effective lipid order parameter.

**Acknowledgements** This work was supported by Project No. LO1211, Materials Research Centre at FCH BUT-Sustainability and Development (National Programme for Sustainability I, Ministry of Education, Youth and Sports of the Czech Republic).

## Compliance with ethical standards

**Conflict of interest** The authors declare that they have no conflict of interest.

## References

- Gu L, Faig A, Abdelhamid D, Uhrich K (2014) Sugar-based amphiphilic polymers for biomedical applications: from nanocarriers to therapeutics. *Acc Chem Res* 47:2867–2877. doi:10.1021/ar4003009
- Sapsford KE, Algar WR, Berti L, Gemmill KB, Casey BJ, Oh E, Stewart MH, Medintz IL (2013) Functionalizing nanoparticles with biological molecules: developing chemistries that facilitate nanotechnology. *Chem Rev* 113:1904–2074. doi:10.1021/cr300143v
- Bode C, Trojan L, Weiss C, Kraenzlin B, Michaelis U, Teifel M, Alken P, Michel MS (2009) Paclitaxel encapsulated in cationic liposomes: a new option for neovascular targeting for the treatment of prostate cancer. *Oncol Rep* 22:321–326. doi:10.3892/or\_00000440
- Campbell RB, Balasubramanian SV, Straubinger RM (2001) Phospholipid-cationic lipid interactions: influences on membrane and vesicle properties. *Biochim Biophys Acta Biomembr* 1512:27–39. doi:10.1016/S0005-2736(01)00290-5
- Thevenot J, Troutier AL, David L, Delair T, Ladavière C (2007) Steric stabilization of lipid/polymer particle assemblies by poly(ethylene glycol)-lipids. *Biomacromolecules* 11:3651–3660. doi:10.1021/bm700753q
- Thevenot J, Troutier AL, Putaux JL, Delair T, Ladavière C (2008) Effect of the polymer nature on the structural organization of lipid/polymer particle assemblies. *J Phys Chem B* 112:13812–13822. doi:10.1021/jp805865r
- Chen Y, Bothun GD (2011) Cationic gel-phase liposomes with “decorated” anionic SPIO nanoparticles: morphology, colloidal, and bilayer properties. *Langmuir* 27:8645–8652. doi:10.1021/la2011138
- Troutier AL, Delair T, Pichot C, Ladavière C (2005) Physicochemical and interfacial investigation of lipid/polymer particle assemblies. *Langmuir* 21:1305–1313. doi:10.1021/la047659t
- Troutier AL, Véron L, Delair T, Pichot C, Ladavière C (2005) New insights into self-organization of a model lipid mixture and quantification of its adsorption on spherical polymer particles †. *Langmuir* 21:9901–9910. doi:10.1021/la050796l
- Parasassi T, De Stasio G, D’Ubaldo A, Gratton E (1990) Phase fluctuation in phospholipid membranes revealed by Laurdan fluorescence. *Biophys J* 57:1179–1186. doi:10.1016/S0006-3495(90)82637-0
- Chong PL, Wong PT (1993) Interactions of Laurdan with phosphatidylcholine liposomes: a high pressure FTIR study. *Biochim Biophys Acta* 1149:260–266. doi:10.1016/0005-2736(93)90209-I
- Parasassi T, Krasnowska EK, Bagatolli L, Gratton E (1998) Laurdan and Prodan as polarity-sensitive fluorescent membrane probes. *J Fluoresc* 8:365–373. doi:10.1023/A:1020528716621
- Bondar OP, Rowe ES (1999) Preferential interactions of fluorescent probe Prodan with cholesterol. *Biophys J* 76:956–962. doi:10.1016/S0006-3495(99)77259-0
- Sanchez SA, Triccerri MA, Gunther G, Gratton E (2007) Laurdan generalized polarization: from cuvette to microscope. In: Méndez-Vilas A, Diaz J (eds) *Modern research and educational topics in microscopy*. Formatex, Madrid, pp. 1007–1014
- Muller JM, Ginkel G, Faassen EE (1996) Effect of lipid molecular structure and gramicidin a on the Core of lipid vesicle bilayers. A

- time-resolved fluorescence depolarization study †. *Biochemistry* 35:488–497. doi:10.1021/bi951409h
16. Ghosh YK, Indi SS, Bhattacharya S (2001) Thermal lipid order–disorder transitions in mixtures of cationic cholesteryl lipid analogues and dipalmitoyl phosphatidylcholine membranes. *J Phys Chem B* 105:10257–10265. doi:10.1021/jp003940e
  17. Repáková J, Čapková P, Holopainen JM, Vattulainen I (2004) Distribution, orientation, and dynamics of DPH probes in DPPC bilayer. *J Phys Chem B* 108:13438–13448. doi:10.1021/jp048381g
  18. Kaiser RD, London E (1998) Location of diphenylhexatriene (DPH) and its derivatives within membranes: comparison of different fluorescence quenching analyses of membrane depth †. *Biochemistry* 37:8180–8190. doi:10.1021/bi980064a
  19. Fraňová M, Repáková J, Čapková P, Holopainen JM, Vattulainen I (2010) Effects of DPH on DPPC–cholesterol membranes with varying concentrations of cholesterol: from local perturbations to limitations in fluorescence anisotropy experiments. *J Phys Chem B* 114:2704–2711. doi:10.1021/jp908533x
  20. Kakehi K, Kinoshita M, Yasueda S (2003) Hyaluronic acid: separation and biological implications. *J Chromatogr B* 797:347–355. doi:10.1016/S1570-0232(03)00479-3
  21. Velema J, Kaplan D (2006) Biopolymer-based biomaterials as scaffolds for tissue engineering. *Adv Biochem Eng Biotechnol* 102:187–238. doi:10.1007/10\_013
  22. Kablik J, Monheit GD, Yu L, Chang G, Gershkovich J (2009) Comparative physical properties of hyaluronic acid dermal fillers. *Dermatol Surg* 35:302–312. doi:10.1111/j.1524-4725.2008.01046.x
  23. Huang SL, Ling PX, Zhang TM (2007) Oral absorption of hyaluronic acid and phospholipids complexes in rats. *World J Gastroenterol* 13:945–949. doi:10.3748/WJG.v13.i6.945
  24. Pasquali-Ronchetti I, Quagliano D, Mori G, Bacchelli B, Ghosh P (1997) Hyaluronan–phospholipid interactions. *J Struct Biol* 120:1–10. doi:10.1006/jsbi.1997.3908
  25. Heatley F, Scott JE (1988) A water molecule participates in the secondary structure of hyaluronan. *Biochem J* 254:489–493. doi:10.1042/bj2540489
  26. Crescenzi V, Taglienti A, Pasquali-Ronchetti I (2004) Supramolecular structures prevailing in aqueous hyaluronic acid and phospholipid vesicles mixtures: an electron microscopy and rheometric study. *Colloid Surf A* 245:133–135. doi:10.1016/j.colsurfa.2004.06.030
  27. Harris FM, Best KB, Bell JD (2002) Use of laurdan fluorescence intensity and polarization to distinguish between changes in membrane fluidity and phospholipid order. *Biochim Biophys Acta* 1565:123–128. doi:10.1016/S0005-2736(02)00514-X
  28. Troup GM, Wrenn SP, Apel-Paz M, Doncel GF, Vanderlick TK (2006) A time-resolved fluorescence diphenylhexatriene (DPH) anisotropy characterization of a series of model lipid constructs for the sperm plasma membrane. *Industrial* 45:6939–6945. doi:10.1021/ie058084d
  29. Heyn MP (1979) Determination of lipid order parameters and rotational correlation times from fluorescence depolarization experiments. *FEBS Lett* 108:81–87. doi:10.1016/0014-5793(79)80564-5
  30. Lakowicz JR (2006) Principles of fluorescence spectroscopy, 3rd edn. Springer, New York
  31. Gurtovenko AA, Patra M, Karttunen M, Vattulainen I (2004) Cationic DMPC/DMTAP lipid bilayers: molecular dynamics study. *Biophys J* 86:3461–3472. doi:10.1529/biophysj.103.038760
  32. Olżyńska A, Jurkiewicz P, Hof M (2008) Properties of mixed cationic membranes studied by fluorescence solvent relaxation. *J Fluoresc* 12:925–928. doi:10.1007/s10895-008-0321-6
  33. Gasperini AAM, Puentes-Martinez XE, Balbino TA, et al (2015) Association between cationic liposomes and low molecular weight hyaluronic acid. *Langmuir* 31:3308–3317. doi:10.1021/la5045865